

# Entanglement Degree Characterization of Spontaneous Parametric-Down Conversion Biphotons in Frequency Domain

Giorgio Brida<sup>1</sup>, Valentina Caricato<sup>1,2</sup>, Marco Genovese<sup>1</sup>, Marco Gramegna<sup>1</sup>, Mikhail V. Fedorov<sup>3</sup>, and Sergey P. Kulik<sup>4</sup>

<sup>1</sup> I.N.R.I.M. - Istituto Nazionale di Ricerca Metrologica, Turin, Italy

<sup>2</sup> Department of Physics, Politecnico of Turin, Turin, Italy  
v.caricato@inrim.it, valentina.caricato@polito.it

<sup>3</sup> A.M.Prokhorov General Physics Institute, Russian Academy of Science, Moscow, Russia

<sup>4</sup> Faculty of Physics, M.V.Lomonosov Moscow State University, Moscow, Russia

**Abstract.** We present an experiment addressed to verify the validity of the entanglement quantifier  $R$ , defined as the ratio between single counts and coincidence distribution width for pure biphoton states generated by short pump pulses. We demonstrate that this ratio can be efficient to estimate entanglement degree in frequency domain. Our work has been performed with a femto second pulsed laser pump addressed to a  $\text{LiIO}_3$  crystal generating correlated biphotons through collinear degenerate type-I SPDC. To study the dependence of  $R$  on the length of the crystal we performed two sequence of measurements for each crystal firstly with a 10 mm and then with a 5 mm.

**Keywords:** Entanglement, biphotons, SPDC.

## 1 Introduction

In the framework of quantum mechanics and quantum optics, entanglement is a powerful resource for developing quantum technologies [1], such as quantum communication, q-calculus, q-imaging, q-metrology, etc. For this reason it is very important to define a precise and easy-implementable method for characterizing entanglement properties. In literature there are several measures that quantify entanglement of quantum bipartite states both in discrete and continuous variables [2]; we want to cite as some examples the Schmidt rank, entropy, concurrence, etc. From a theoretical point of view the density matrix that describes a precise state of bipartite system is useful to evaluate all these quantifiers. On the other side from an experimental point of view a quantum tomography procedure (either complete or reduced) would be necessary [3]. In the case of high-dimensional systems this procedure requires a number of measurements that increases quadratically with the dimension of Hilbert space. Following these considerations, an innovative and alternative method is to analyze and develop

links between entanglement and measurable quantities related to the quantum state, defining precise parameters. For pure biphoton states one of these parameters is the Fedorov's parameter [4]  $R_q$  (where  $q$  denotes an arbitrary space, e.g. frequency or spatial one), defined as the ratio of the single-particle and coincidence distributions widths in  $q$ -space. The advantage of this parameter is that can be rather easily measured at variance with all other entanglement quantifiers. A qualitative approach to  $R_q$  follows from entropy : high entanglement leads to a better knowledge about composite bipartite system (narrower coincidence distribution) and a worse knowledge about individual subsystem(s) (wider single-particle distribution). This clear physical meaning makes  $R_q$  to be an extremely useful tool for entanglement control. It has been proved [4] that for bipartite states, described by a double-Gaussian wave function, the parameter  $R$  coincides exactly with the Schmidt number  $K$ . Also, if we consider special classes of non-double-Gaussian wave functions like those describing Spontaneous Parametric Down-Conversion (SPDC) their values remain quite close as well. This is true both for continue and discrete variables. Recently the  $R$  parameter has been successfully applied for demonstrating a very strong entanglement anisotropy in spatial distributions of biphotons [5].

### 1.1 Aim of the Paper

In this proceeding we present in detail an experimental work devoted to verify the operational entanglement quantifier  $R$  applied to the study of two-photon states entangled in frequency domain [6]. We want to demonstrate that the measure of  $R$  is an efficient alternative to other quantifiers like for example (in specific experiments) the measure of the visibility of interference pattern that can provide some knowledge about entanglement [7]. It is known that two-photon states belong to a multi-dimensional Hilbert space and can possess an extremely high entanglement degree (up to several hundreds) that makes them very perspective in applications of quantum information and quantum communication. It is important to emphasize that in this work our consideration are restricted to purely spectral entanglement. This means that we consider only photons propagating along the pump axis. In our experiment this condition has been realized inserting some very thin slits (50  $\mu\text{m}$  width) in front of detectors in the focal plane of photons emitted from a  $\text{LiIO}_3$  crystal. An opposite case, where the photon frequencies are fixed but directions of their propagation can change, has been investigated earlier [5].

## 2 Theoretical Considerations

We consider the pump described by a sequence of short Fourier-limited pulses, which provides conditions for generating pure biphoton states characterized by a wave function. We are interesting in type-I degenerate collinear SPDC where the wave function  $\Psi$ , depending only on frequencies of emitted signal and idler photons  $\omega_1$  and  $\omega_2$ , is given by [8,9]

$$\Psi(\nu_1, \nu_2) \propto \exp\left(-\frac{(\nu_1 + \nu_2)^2 \tau^2}{8 \ln 2}\right) \times \text{sinc}\left\{\frac{L}{2c} \left[A(\nu_1 + \nu_2) - B \frac{(\nu_1 - \nu_2)^2}{\omega_p}\right]\right\} \quad (1)$$

The first term in the wave function is a Gaussian exponent that describes the pump spectral amplitude. The pump-pulse duration is  $\tau$ ,  $L$  is the length of the crystal,  $\nu_1$  and  $\nu_2$  are deviations of the frequencies of the signal and idler photons  $\omega_{1,2}$  from the central frequencies  $\omega_1^{(0)} = \omega_2^{(0)} = \omega_p/2$ ,  $|\nu_{1,2}| \ll \omega_p$ ,  $\omega_p$  being the central frequency of the pump spectrum.  $A$  and  $B$  are the temporal walk-off and dispersion constants

$$A = c \left( k'_p(\omega)|_{\omega=\omega_p} - k'_1(\omega)|_{\omega=\omega_p/2} \right) = c \left( \frac{1}{v_g^{(p)}} - \frac{1}{v_g^{(o)}} \right)$$

$$B = \frac{c}{4} \omega_p k''_1(\omega)|_{\omega=\omega_p/2} . \quad (2)$$

$v_g^{(p)}$  and  $v_g^{(o)}$  are the group velocities of the pump and ordinary waves, and  $k_1$  and  $k_p$  are the wave vectors of signal and pump photons.

We want to stress that in a more general case both linear and quadratic terms in the argument of the sinc-function in (1) are important and none of them can be eliminated. The sinc-function cannot be substituted by any Gaussian function and, for this reason, the wave function (1) is considered as a non-double-Gaussian one. We use the wave function (1) to estimate the theoretical coincidence and single-particle biphoton spectra. It is important to notice that these spectra are significantly different in the cases of short and long pump pulses. It has been defined the control parameter separating the regions of short and long pulses and it is expressed by [8]

$$\eta = \frac{\Delta\nu_1 \text{sinc}}{\Delta\nu_1 \text{pump}} \approx 2 \frac{c\tau}{AL} = \frac{2\tau}{L/v_g^{(p)} - L/v_g^{(o)}} . \quad (3)$$

i.e., it changes linearly with the pump-pulse duration and decreases if the length of the crystal increases. For a fixed length of the crystal pump pulses are short if  $\eta \ll 1$  and long if  $\eta \gg 1$  and, typically,  $\eta \sim 1$  at  $\tau \sim 1$  ps. The two limits  $\eta \ll 1$  and  $\eta \gg 1$  correspond to a pump spectral amplitude expressed as a function of  $\nu_{1,2}$ , much narrower and much wider than the sinc-function in (1). The parameter (3) contains factors that can be easily controlled in the experiment of this paper, namely the length of the crystal and the pump pulse duration. The choose of a particular crystal with specific dispersion properties can act on the longitudinal walk-off effect expressed in the term  $A$ . Let's focus our attention on the short pump pulses  $\eta \ll 1$ : the FWHM of the coincidence and single-particle spectra were found analytically to be given by [8]

$$\Delta\omega_c = \frac{5.56 c}{AL}, \quad \Delta\omega_s = \sqrt{\frac{2A \ln(2) \omega_p}{B\tau}} . \quad (4)$$

The first formula follows directly from (1) whereas the second one requires for its derivation a preliminary integration of  $|\Psi(\nu_1, \nu_2)|^2$ , for example over  $\nu_2$  [8]. For long pump pulses  $\eta \gg 1$ , the coincidence and single-particle spectral widths have the form [8]

$$\Delta\omega_c = \frac{4 \ln 2}{\tau}, \quad \Delta\omega_s = \sqrt{\frac{2.78 c \omega_0}{L B}}. \quad (5)$$

We use equations (4) and (5) to find the expression of the parameter  $R(\eta)$  in regions of short and long pulses as :

$$R(\eta) = \frac{\Delta\omega_s}{\Delta\omega_c}. \quad (6)$$

In the intermediate region ( $\eta \sim 1$ ) the  $R(\eta)$  can be determined by a quadratic interpolation [8]

$$R(\eta) \approx \sqrt{R_{\text{short}}^2 + R_{\text{long}}^2} = 0.75 \frac{A}{\sqrt{B}} \sqrt{\frac{L}{\lambda_0} \sqrt{\eta^2 + \frac{1}{\eta}}} = 55 \sqrt{\eta^2 + \frac{1}{\eta}}. \quad (7)$$

The function  $R(\eta)$  (7) is plotted in Fig. 1 together with the Schmidt number  $K(\eta)$ . The latter was calculated numerically by Silberhorn and Mauerer [10] who demonstrated that, in the region of short and long pulses, the phase of the wave function does not affect the Schmidt number.

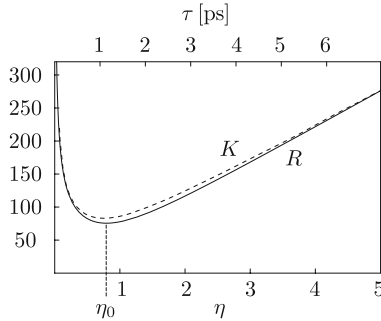


**Fig. 1.** Quantifiers calculated analytically ( $R$  [8]) and numerically ( $K$  [10]) for  $\text{LiIO}_3$  crystal of a length  $L = 0.5$  cm and the pump wavelength  $\lambda_p = 400$  nm

It is visible from the picture that the functions  $R(\eta)$  and  $K(\eta)$  are very close each other, and this confirms the validity of the experimentally measurable parameter  $R$  for quantifying the degree of entanglement of biphoton states characterized by a non-double-Gaussian wave function of the form (1). From the previous theoretical considerations the degree of spectral entanglement reaches very high values in the whole range of pump-pulse durations when we are sufficiently far from the minimum localized at  $\eta \sim 1$  or  $\tau \sim 1$  ps.

### 3 Experimental Set Up and Results

The experiment here described was performed in fs pulsed regime with a Mode-Locked Titanium-Sapphire laser at a working wavelength of  $\lambda_{IR} = (795.0 \pm$

0.1) nm with a  $\Delta\lambda_{IR} = (5.9 \pm 0.1)$  nm. After doubling in frequency by second harmonic generation we obtained a pump of  $\lambda_p = (397.5 \pm 0.2)$  nm and  $\Delta\lambda_p = (1.8 \pm 0.1)$  nm, corresponding to a pulse duration of  $\tau = (186 \pm 30)$  fs. We estimated the beam waist to be smaller than 2 mm. The pump spectrum observed on a spectrometer analyzer showed an IR component @ 795 nm still present in the pump so we inserted in the beam two quartz prisms oriented at the Brewster's angle to reduce the fundamental residual as much as possible. In order to study the dependence of the  $R(\eta)$  parameter on the crystal length  $L$ , we performed two different sequences of measurements, one addressing the pump beam to a 10 mm  $\text{LiIO}_3$  the other to a 5 mm crystal. With the correct phase matching angle the horizontally polarized beam generated two vertically polarized photons through the non linear optic process known as type I collinear SPDC. A couple of UV mirrors was inserted after the crystal to eliminate the UV pump, and biphotons produced were divided by a non polarizing beam-splitter and sent to two photodetection apparatuses consisting of red glass filters and two single photo-detectors (SPAD: Perkin-Elmer SPCM-AQR-15). The photodetectors are characterized by a photon efficiency variable with the wavelength. Our working range was from 700 nm to 900 nm (Fig. 2).

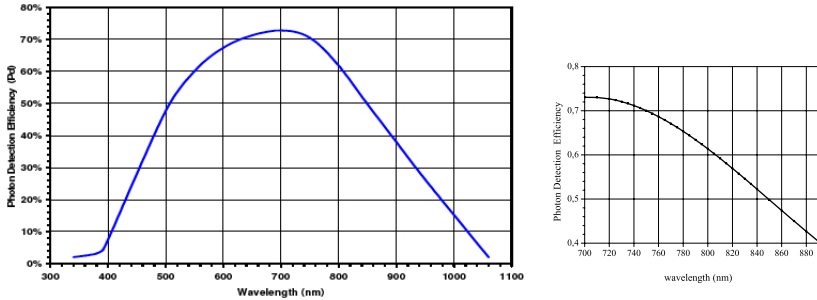


**Fig. 2.** Photon Detection Efficiency of Perkin-Elmer detectors and a detail in the range from 700 nm to 900 nm

In front of each detector it was placed a monochromator with a variable spectral resolution. A lens with a focal distance of 20 cm and with a diameter of 2.5 cm was fixed 135 cm far from the crystal in order to focalize the light inside each monochromator and a couple of lenses with the same focal distance were placed on the output of the monochromators. It is worth to mention that the lenses placed at this large distance, with this small diameter, have been worked as selective tool on the spatial modes of biphotons allowing to collect a single spatial mode in the monochromators.

All experiments were performed as a sequence of corresponding measurements of spectral distributions both in single counts and coincidences. When the best phase matching conditions had been found the measure of the coincidence distribution was performed fixing one of the two monochromators at the central

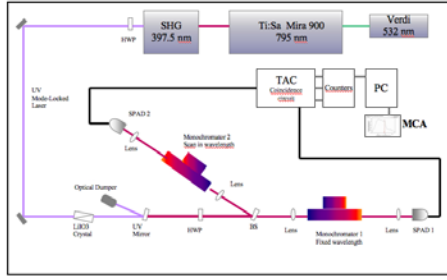


**Fig. 3.** Experimental set up: a duplicated titanium sapphire laser beam pumps a  $\text{LiIO}_3$  crystal generating collinear SPDC. After a Half Wave Plate (HWP) the biphotons are split on a beam-splitter (BS) and fed to SPAD detectors, whose output feeds Time-to Amplitude Converter (TAC), counters and Multi Channel Analyzer (MCA).

wavelength of SPDC (795 nm) and scanning the other one in a range around this value. The same procedure has been applied for the single counts distribution.

### 3.1 Measure with a 10 mm $\text{LiIO}_3$ Crystal

The first series of measurements was performed with a 10 mm  $\text{LiIO}_3$  crystal. To measure the coincidence distribution we have used monochromators with 0.2 nm resolution for scanning the signal wavelength. For each wavelength we got three measurements of the number of counts for real and accidental coincidence distributions. Each measurement was performed in an acquisition time of 100 s and we selected on the multichannel analyzer a window of 670 channels (i.e. 1,64 ns) for both distributions. After correcting the counts for the accidental ones, we evaluated the average and the standard deviation, then our measurements were corrected taking into account the efficiency of the detectors and finally the plot was normalized. Subsequently experimental points were fitted by a gaussian distribution in order to have for the distribution an expected value for the FWHM with its uncertainty. In this configuration we obtained a narrow peak with  $\Delta\lambda_c = (0.29 \pm 0.03)$  nm (Fig. 4). By a comparison the pump width was 6.2 times larger than the coincidence spectrum.

The spectral distribution of single counts was performed using a monochromator in the transmission arm with a spectral resolution of 1 nm. For this measure we scanned each wavelength five times and we registered counts on one detector for a temporal window of 5 s. To evaluate the background we inserted a HWP cut for 400 nm before the pump in order to rotate the pump polarization from horizontal to vertical: in this way without rotating phase matching angle no correlated photons were produced. We subtracted again the background from the single counts and we evaluated the uncertainty with usual uncertainty propagation formula. Also in this case each value was corrected taking into account the efficiency of the detector for different wavelengths and the plot was finally normalized. We estimated the FWHM of the distribution from the experimental points and we associated the resolution of the CVI monochromator as the uncertainty

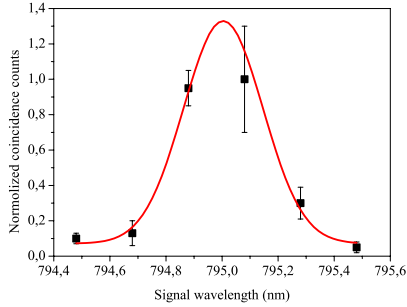


**Fig. 4.** Normalized coincidence distribution for 10 mm length  $\text{LiIO}_3$  sample

on this measure, obtaining the single counts spectral width  $\Delta\lambda_s = (101 \pm 1)$  nm (Fig. 5). It is worth to notice that data present a strong asymmetry of the right wing in the measured spectrum. This effect probably might be caused by loosing in spectral sensitivity of monochromator for long wavelength.

The distribution of single counts is 56 times larger than that of the pump, corresponding to an experimental ratio between widths of the two distributions  $R_\omega = (349 \pm 43)$ . The complete results are listed in the table 1.

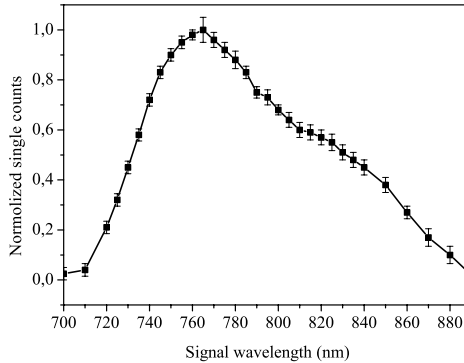


**Fig. 5.** Normalized single counts distribution for 10 mm length  $\text{LiIO}_3$  sample

**Table 1.** Results for 10 mm  $\text{LiIO}_3$  sample

Theory Model	Experimental results
Coincidence Distribution	
$\Delta\lambda_c = 0.32$ nm	$\Delta\lambda_c = (0.29 \pm 0.03)$
Single Counts Distribution	
$\Delta\lambda_s = 100$ nm	$\Delta\lambda_s = (101 \pm 1)$ nm
$R$ -Quantifier	
$R_\omega \approx R_\lambda \approx 316$	$R_\omega \approx R_\lambda \approx (349 \pm 43)$

### 3.2 Measure with a 5 mm LiIO<sub>3</sub> Crystal

The same sequence of measurements, single counts and coincidence distribution, has been performed with a 5 mm length crystal obtaining for the coincidence distribution a  $\Delta\lambda_c = (0.64 \pm 0.06)$  nm. The results are plotted in Fig. 6.

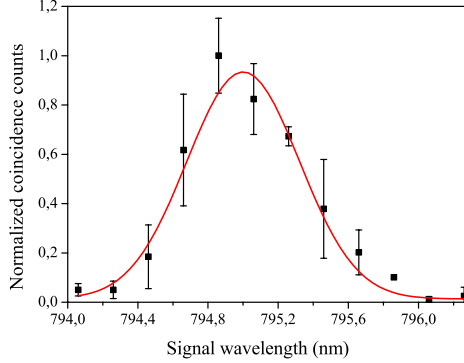


**Fig. 6.** Normalized coincidence distribution for 5 mm length LiIO<sub>3</sub> sample

The single counts distribution has now a width  $\Delta\lambda_s = (115 \pm 1)$  nm. It is shown in Fig. 7 including the correction due to the detectors efficiency. This second set of measurements corresponds to  $R_\omega = (179 \pm 18)$ . It is important to notice that the pulse duration of the pump did not change respect to the previous measurements with the 10 mm crystal and we can observe that, in this case, the pump spectra is 2.8 times wider than the coincidence spectrum whereas the single counts distribution is 64 times larger than the width of the pump, in agreement with what expected from theory. Corresponding results are listed in table 2.

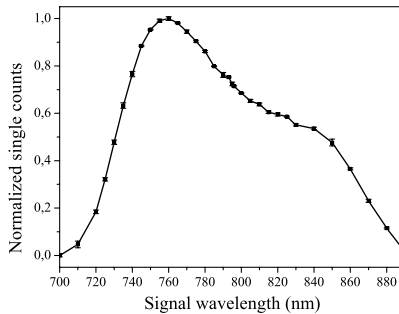


**Fig. 7.** Normalized single counts distribution for 5 mm length LiIO<sub>3</sub> sample



**Table 2.** Results for 5 mm LiIO<sub>3</sub> sample

Theory Model	Experimental results
Coincidence Distribution	
$\Delta\lambda_c = 0.63$ nm	$\Delta\lambda_c = (0.64 \pm 0.06)$
Single Counts Distribution	
$\Delta\lambda_s = 100$ nm	$\Delta\lambda_s = (115 \pm 1)$ nm
<i>R</i> -Quantifier	
$R_\omega \approx R_\lambda \approx 158$	$R_\omega \approx R_\lambda \approx (179 \pm 18)$

## 4 Conclusions and Future Plans

In this work we have experimentally verified the validity of the *R*-quantifier as an efficient tool to estimate entanglement degree in frequency domain for pure biphoton states generated by short pump pulses. More in detail, our work has been performed with a femto-second pulsed laser and the parameter we have changed to study the validity of this approach is the length of the LiIO<sub>3</sub> crystal. It is worth to notice that a variation in the  $\eta$  parameter can be realized by changing either the length  $L$  of the crystal or the pulse duration  $\tau$ . However, working on the pulse duration in a wide range with the same laser results quite difficult because it leads to a loose of power and then decreases the production of biphotons after the crystal. Nevertheless, our results show a good agreement between the measured and predicted shapes of the curve shown at Fig. 1 and this completely confirms the adequacy of the *R*-quantifier approach. We observe that by doubling the sample length one doubles the entanglement degree for the short pump pulse regime of SPDC. Unfortunately, if we still decrease the length of the crystal we reduce too much the biphoton flux and reach the minimum of the  $R(\eta)$  becomes quite difficult. We remind that the method of measurement of *R* in frequency domain implies that other degrees of freedom of biphotons should be fixed. Concerning the spatial distribution of photon pairs emitted by crystal, these modes can be selected with the help of small pinholes. On the other side if we want to measure *R* in spatial variables fixing the frequencies of both photons, we need some very narrow-band filters [5]. We would like to mention also that a measurement of spectral widths can be done by transforming spectrum in time difference through a fiber [11]. Finally we wish to acknowledge the work of [12] that is directly related to the subject of this work and was submitted right after we finished it.

**Acknowledgments.** This work has been partially supported by MIUR (PRIN 2007FYETBY), Regione Piemonte (E14), "San Paolo foundation", RFBR (08-02-12091) and NATO Grant (CBP.NR.NRCL 983251).

## References

1. Genovese, M.: Research on hidden variable theories: A review of recent progresses. Phys. Rep. 413, 319–396 (2005)
2. Bengtsson, I., Życzkowski, K.: Geometry of Quantum States. Cambridge Univ. Press, Cambridge (2006)

3. Zavatta, A., et al.: Tomographic reconstruction of the single-photon Fock state by high-frequency homodyne detection. *Phys. Rev. A* 70, 053821 (6 pages) (2004)
4. Fedorov, M.V., Efremov, M.A., Volkov, P.A., Eberly, J.H.: Short-pulse or strong-field breakup processes: a route to study entangled wave packets. *J. Phys. B: At. Mol. Opt. Phys.* 39, S467–S483 (2006)
5. Fedorov, M.V., Efremov, M.A., Volkov, P.A., Moreva, E.V., Straupe, S.S., Kulik, S.P.: Anisotropically and High Entanglement of Biphoton States Generated in Spontaneous Parametric Down-Conversion. *Phys. Rev. Lett.* 99, 063901 (4 pages) (2007)
6. Brida, G., Caricato, V., Genovese, M., Gramegna, M., Fedorov, M.V., Kulik, S.P.: Characterization of Spectral Entanglement of Spontaneous Parametric-Down Conversion Biphotons, <http://arxiv.org/abs/0904.3009>
7. Kim, Y., et al.: Temporal indistinguishability and quantum interference. *Phys. Rev. A* 62, 43820 (4 pages) (2000); Jeronimo-Moreno, Y., U'Ren, A.B.: Control, measurement, and propagation of entanglement in photon pairs generated through type-II parametric down-conversion. *Phys. Rev. A* 79, 033839 (14 pages) (2009)
8. Mikhailova, Y.M., Volkov, P.A., Fedorov, M.V.: Biphoton wave packets in parametric down-conversion: Spectral and temporal structure and degree of entanglement. *Phys. Rev. A* 78, 062327 (17 pages) (2008)
9. Keller, T.E., Rubin, M.H.: Theory of two-photon entanglement for spontaneous parametric down-conversion driven by a narrow pump pulse. *Phys. Rev. A* 56, 1534–1541 (1997)
10. Maurer, W., Silberhorn, C.: Numerical Analysis of Parametric Downconversion. In: *AIP Conf. Proc: Quantum Communication, Measurement and Computing (QCMC 2008)*, vol. 1110, pp. 220–223 (2009)
11. Brida, G., Chekhova, M.V., Genovese, M., Gramegna, M., Krivitsky, L.A.: Dispersion Spreading of Biphotons in Optical Fibers and Two-Photon Interference. *Phys. Rev. Lett.* 96, 143601 (4 pages) (2006); Brida, G., Genovese, M., Krivitsky, L.A., Chekhova, M.V.: Interference structure of two-photon amplitude revealed by dispersion spreading. *Phys. Rev. A* 75, 015801 (4 pages) (2007)
12. Avenhaus, M., Chekova, M.V., Krivitsky, L.A., Leuchs, G., Silberhorn, C.: Experimental verification of high spectral entanglement for pulsed waveguided spontaneous parametric down-conversion. *Phys. Rev. A* 79, 043836 (5 pages) (2009)